Three-dimensional radiation transfer modeling in a dicotyledon leaf

Yves M. Govaerts, Stéphane Jacquemoud, Michel M. Verstraete, and Susan L. Ustin

The propagation of light in a typical dicotyledon leaf is investigated with a new Monte Carlo ray-tracing model. The three-dimensional internal cellular structure of the various leaf tissues, including the epidermis, the palisade parenchyma, and the spongy mesophyll, is explicitly described. Cells of different tissues are assigned appropriate morphologies and contain realistic amounts of water and chlorophyll. Each cell constituent is characterized by an index of refraction and an absorption coefficient. The objective of this study is to investigate how the internal three-dimensional structure of the tissues and the optical properties of cell constituents control the reflectance and transmittance of the leaf. Model results compare favorably with laboratory observations. The influence of the roughness of the epidermis on the reflection and absorption of light is investigated, and simulation results confirm that convex cells in the epidermis focus light on the palisade parenchyma and increase the absorption of radiation.

Key words: Three-dimensional dicotyledon leaf structure, leaf optical properties, leaf spectrum, ray-tracing, bidirectional reflectance, radiation transfer model.

1. Introduction

By providing energy for photosynthesis and other physiological processes such as morphogenesis, solar radiation largely regulates the growth and development of plants.[1] The interaction between the photosynthesizing organs of the plant and light has been studied for many years, first in the field of photobiology, later as part of physiological ecology,[2] and more recently to support remote-sensing applications of vegetated surfaces.[3] Indeed, the retrieval of quantitative information from remote sensing requires analytical tools such as canopy reflectance models to interpret radiative measurements in terms of aeronomical or ecological properties such as leaf biochemistry or canopy architecture.[4] At the spatial scale and resolution of optical spaceborne remote-sensing observations, leaves are the principal absorbing and scattering elements of live green plant canopies.[5] The proper understanding of the processes of radiation transfer in leaf tissues is essential to comprehend the functioning of leaves but also to take full advantage of remote-sensing measurements.

The attenuation of light inside plant leaves results from complex absorption and scattering processes controlled by the biochemical composition and morphological features of the various tissues. The epidermis plays an important role in determining the overall bidirectional reflectance of the leaf whereas the chlorophyll amount in the parenchyma and spongy mesophyll control the level of light absorption. Although the leaf spectral properties of various plants are relatively well described in the literature, only a few measurements of the directional dependency of leaf reflectance and transmittance have been reported, and then for only a handful of species.

Over the last 50 years, various authors have examined the influence of biochemical composition and anatomical features on leaf optical properties.[6] However, the rapid development of computer-based models since the late 60's has allowed significant quantitative progress in the understanding of the interaction of light with plant leaves. The range of models that have been developed to address this scientific problem has been recently reviewed.[7] Of the various models that have been proposed so far, the ray-tracing approach is the only one that can account

Y. M. Govaerts and M. M. Verstraete are with the Space Applications Institute, TP 440, Commission of the European Communities Joint Research Centre, I-21020 Ispra (Varese), Italy. S. Jacquemoud is with Laboratoire Environnement et Développement, Université Paris 7, Case Postale 7071, Place Jussieu 2, F-75251 Paris Cedex 05, France. S. L. Ustin is with the Department of Land, Air, and Water Resources, University of California, Davis, Davis, California 95616.

Received 17 November 1995; revised manuscript received 30 April 1996.

0003-6935/96/06585-14$10.00/0

for the full three-dimensional complexity of the internal leaf structure as it appears in a photomicrograph. The method requires a detailed description of the structure and properties of individual cells, as well as their particular spatial arrangement inside tissues. Once each of the leaf constituents (cell walls, cytoplasm, pigments, air cavities, etc.) has been assigned specific optical properties, it is possible to simulate the propagation of individual light rays incident on the leaf surface on the basis of classical physical laws such as reflection, refraction, and absorption. Statistically representative values of the leaf radiative properties of interest are estimated from an analysis of a sufficiently large number of rays.

This ray-tracing technique has already been applied for a number of scales. The first studies were performed at the cell level,[8,9] in particular to investigate the role of epidermal cells on the path of the incident radiation beam: the convex cells of some plants appear to act as lenses to focus light within the upper region of the palisade parenchyma, which contains many chloroplasts adapted to high light levels. This feature has been largely understood as an adaptation to the low light environment on the tropical forest floor,[10] although it has also been suggested that epidermal lenses could increase the absorption of light at low Sun angles among cultivated plants (*Medicago sativa*).[11] On a larger scale, research has been pursued to gain a better understanding of the transmission of light through entire leaves. In one such case, the complete leaf structure was described by 100 circular arcs, whereas leaf composition was restricted to two media: intercellular airspace and cell walls, each characterized by their refractive index.[12] This model was used to simulate the specular and diffuse reflection of light at the cell walls but led to an underestimation of the reflectance and an overestimation of the transmittance in the near-infrared spectral region. It was later found that the estimation of leaf reflectance and transmittance was improved by adding two more media to the model (the cytoplasm and chloroplasts), thereby increasing the internal scattering of light.[13]

In all these cases, the absorption phenomena that characterize leaf optical properties outside the near-infrared region have been ignored. Moreover, all these models described leaves as two-dimensional objects, although the three-dimensional structure of these organs is important to their physiological function (e.g., for CO_2, H_2O, O_2 diffusion) and to light scattering.[14,15] As a matter of fact, three-dimensional radiation transfer models are the only ones capable of describing the heterogeneity of the media and its effect on the propagation of light. In this paper we used a recently developed three-dimensional light scattering model to describe the transfer of radiation inside a dicotyledon leaf as a function of its internal structure and morphological properties. This model aims at (1) representing as faithfully as possible the internal structure of the leaf to improve the interpretation of reflectance measurements in terms of vegetation biophysical properties, and (2) evaluating whether the representation of leaves as layers of cells, together with the classical principles of optics, is sufficient to account for the available measurements of leaf optical properties. In Section 2 we describe a general method to build a virtual plant leaf that is realistic in terms of both plant anatomy and physiology and is suitable for the ray-tracing model. In Section 3 we outline the design of a virtual typical dicotyledon leaf, paying special attention to its structural and optical properties. The ray-tracing model used to simulate the interaction of light rays with this leaf (RAYTRAN) is briefly described in Section 4. In Section 5 we compare various model results with observed leaf spectral and bidirectional properties.

2. Concept and Methods

Ray-tracing techniques require a detailed description of the leaf geometric properties as well as knowledge of the mechanisms involved in the scattering and absorption of light at different levels of organization and at different wavelengths. Although modeling leaf anatomy in two dimensions was relatively easy, the generation of a three-dimensional leaf structure is much more challenging. One major issue is the general lack of information on the structure of leaf tissues.[16] First, in real tissues, cells present a great diversity of shape, size, and arrangement. They are generally enclosed in leaf tissues that are agglomerates of neighboring cells in close contact.[17] Second, compared with other cellular solids, plant cells do not completely fill the available space: intercellular air may occupy a significant volume fraction, which varies with plant species, leaf tissue, as well as environmental conditions (e.g., Sun-illuminated or Sun-shaded leaves, hydrophytic or xerophytic leaves). Only three-dimensional models could provide a meaningful representation of the spatial structure of the leaf.

Various assumptions must be made on the shape and size of the cells and on their spatial arrangement in tissues, if efficient numerical computations are to be performed repetitively. In particular, cells will be represented through simple geometric objects, and tissues by juxtapositions of such objects. The implications of these representations at the cell and tissue levels are now discussed.

A. Schematic Representation of a Leaf Cell

Although plant leaves may present numerous anatomical structures, and leaf cells may vary largely in shape and size according to the foliar tissue type (protective tissue such as the cuticle, conductive tissue such as veins, parenchyma, etc.), basic cell structures are relatively uniform because of common cell functions.[18] Cells are surrounded by a wall and a plasma membrane containing the cytoplasm with several organelles (nucleus, mitochondria, chloroplasts, amyloplasts, endoplasmic reticulum, etc.) and a central vacuole that may occupy as much as 90% of the cell volume. Chloroplasts are found within the cytoplasm of all photosynthesizing cells [Fig. 1(A)].

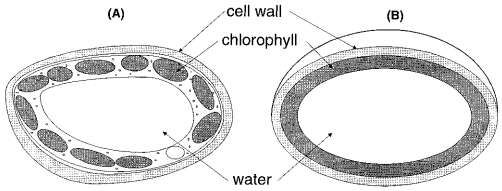

Fig. 1. (A) Schematic representation of a mesophyll leaf cell showing the complexity of the different membranes. (B) For modeling purposes, the internal cell structure is represented as three homogeneous membranes.

All these elements scatter or absorb the light penetrating a plant cell. At all scales where the size of the scattering particles is much greater than the wavelength, refractive-index differences between two different media create optical boundaries. When the particle size is less than or approximately equal to the wavelength, Rayleigh and Mie scattering may occur. Although the dimensions of plant cells with respect to solar wavelengths are too large to induce such phenomena,[19,20] the cytoplasmic organelles, such as chloroplasts, whose size is comparable to optical wavelengths, and large molecules, such as proteins, do scatter light. Absorption results essentially from electronic transitions and vibrations of polyatomic molecules. Electronic transitions mainly involve porphyrin rings in photosynthetic pigments such as chlorophyll; they act as photoreceptors to convert sunlight into chemical energy for the reduction of CO_2 into carbohydrates.[21] Vibrations of polyatomic molecules involve another category of chemical compounds: the most common is water, which fills the vacuole and represents from 40 to 90% of the fresh leaf by weight. Cellulose, hemicellulose, and lignin are other compounds located mainly in the cell walls of all plants, where they act to strengthen and protect plant structures.

Plant cells have been classically modeled as polyhedra.[22,23] The rhombic dodecahedron (ten parallelogram faces) or the tetrakaidecahedron (8 hexagonal faces and 6 square faces), which fill space when assembled as shown in Fig. 2, are commonly used. Although these forms are closely approached or even attained in certain simple and homogeneous plant tissues, they can hardly represent cells of leaf tissues that are not made of regularly packed identical units,

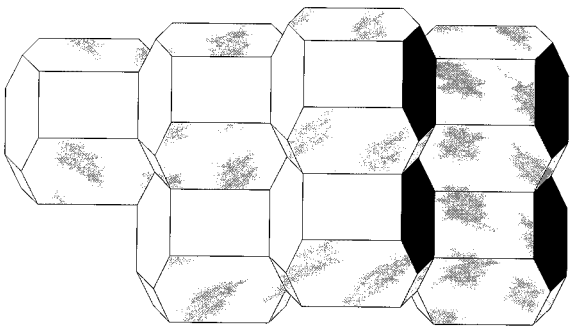

Fig. 2. Seven 14 hedra to show close packing.

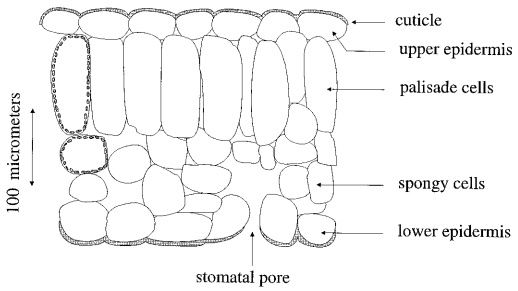

Fig. 3. Schematic transverse section through a dicotyledon leaf indicating the arrangement of tissues. Chloroplasts are drawn in one cell only of both palisade and spongy tissues.

but instead contain cells of different sizes and shapes with differing numbers of faces and edges. In theory, it should be possible to simulate actual cells by defining polyhedra with faces varying in number from 4 to 50 or more.[24] However, multiplying the number of faces tends to smooth the cell shape until it converges to a spherelike volume. Consequently, we decided to simulate cells with primitive objects (spheres, ellipsoids, cylinders, etc.) that can be carved out and assembled using the constructive solid geometry (CSG) method.[25] The current model defines a typical cell as a set of concentric objects, filled with three different media: cell wall material (cellulose, hemicellulose, and lignin), chlorophyll, and water [Fig. 1(B)]. The number of media may be changed. For example, except for stomatal guard cells, cells of the epidermis have only two media instead of three because of the absence of chlorophyll. Each modeled medium is homogeneous: its physical properties are assumed constant in space and isotropic (independent of the direction). Each cell constituent is therefore characterized by a volume, a refractive index, and an absorption coefficient to describe the partitioning of light among the reflected, transmitted, or absorbed contributions. This simplified representation still allows us to take into account the basic cell functions.

B. Schematic Representation of a Leaf Tissue

In real tissues, cells are not isolated but are bound to neighboring cells in multiple directions. They may also be separated by intercellular airspaces. Although the internal structure of plant leaves varies from species to species, the following model is based on the representation of a typical dicotyledon leaf, with the palisade and spongy mesophyll tissues between two layers of epidermal cells as illustrated in Fig. 3.

The epidermis is made up of a single layer of colorless cells, with few if any chloroplasts, and entirely covers both faces of the leaf. Leaf surfaces play a crucial physiological role in protecting these organs from various environmental conditions, such as heat and water stresses, biological threats, etc. As far as radiation transfer is concerned, the main effect of these surfaces is to reflect light unequally in various directions. For example, many leaves exhibit rather

strong specular reflectance under specific conditions. This non-Lambertian behavior has been well documented in the literature, especially at oblique incident angles.[26–28] The light reflected by surfaces in general and by leaves in particular is also often polarized.[29]

Contrary to monocotyledon leaves characterized by a homogeneous parenchyma with few intercellular airspaces, the mesophyll of dicotyledons is characteristically differentiated into a palisade and a spongy mesophyll. Palisade cells are elongated, densely packed, and arranged in one to several layers that contain the largest proportion of chloroplasts. The spongy mesophyll is made up of highly lobed irregularly shaped cells of variable sizes, separated by large intercellular air-filled spaces that facilitate the circulation of gases (CO_2, H_2O, O_2) inside the leaf.[14] Why natural selection has led to this differentiation is still unclear, but the arrangement of cells in space appear to follow precise rules. Specifically, the structure of leaves strongly influences the efficiency of light absorption in plants.[15] The model we describe permits the study of particular questions, such as the role played by the palisade cells in controlling the distribution of light within the leaf. The volume fraction of air-filled spaces, which varies from one leaf tissue to another, may also play an important role in gas diffusion and light scattering. Clearly, the representation of leaf tissues as assemblages of cells made up from elementary volumes should take these elements into account.

3. Construction of a Typical Dicotyledon Leaf

Based on the information in Section 2 one can determine that the leaf internal structure and the optical properties of each of the media constituting the cell elements must both be carefully simulated if the reflectance and transmittance properties of a typical bifacial mesophytic dicotyledon leaf are to be estimated accurately.

A. Cell Membrane Optical and Physical Properties

The spectral variation of the refractive index and the absorption coefficient k of each medium (cell wall, chlorophyll, and water) are both necessary to simulate the scattering and absorption events inside the leaf. The *in vivo* specific absorption coefficient of water[30] has been used; it is similar to that of pure water.[31] Values of the refractive index of water have also been published.[32] For cell walls, the refractive index of leaf material derived by the PROSPECT model[3] and the specific absorption coefficient of cellulose, hemicellulose, and lignin for dry leaves[30] were used. The specific absorption coefficients determined by the same authors for photosynthetic pigments (primarily chlorophyll) were also used (Fig. 4). Although pigment molecules attached to the thylakoid membranes have clumped distributions, we considered a homogeneous distribution within the layer. For practical purposes, as hypothesized before,[33] we assumed that chlorophyll had the same real part of the refractive index as its environment, i.e., as water.

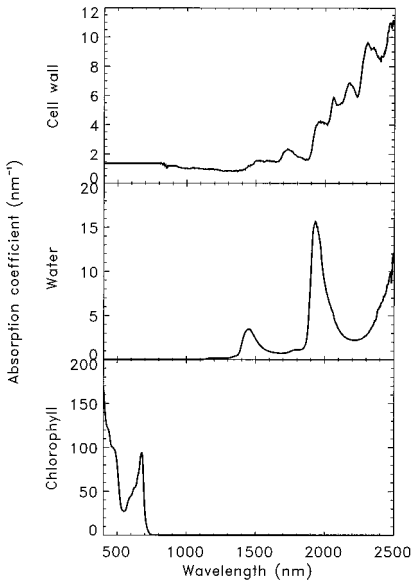

Fig. 4. Absorption coefficient in inverse nanometers of the various cell membranes.

B. Description of the Leaf Internal Structure

The requirements are first, to define the cell shapes, sizes, and their spatial arrangement in different tissues, and second, to derive the equations that characterize the volume of each membrane. These equations are then used to compute the total amounts of the various media in each of the different tissues. The dimensions of the leaf cells have been determined by observations. For example, typical dimensions are 15 μm $\times$ 15 μm $\times$ 60 μm for palisade cells and 18 μm $\times$ 15 μm $\times$ 20 μm for spongy mesophyll and epidermal cells.[19,34] These characteristics have been selected to ensure realistic values of the cell density, i.e., the number of cells per unit area, and thereby the airspace volume. The thickness of the cell membranes is fixed for the cell wall (cellulose and lignin) and the remaining volume is assigned to water and chlorophyll in such a way that these constituents occur in the correct concentrations. The shape, size, and position of the cells have been chosen to ensure that the gross structural and biochemical properties of the leaf are realistic. Table 1 provides further quantitative information on these parameters.

1. Epidermis

We modeled both the upper and lower epidermis as layers of compact ellipsoidal cells. No intercellular spaces are normally present in this particular tissue, which controls gas exchanges between the leaf and its environment through stomatal pores. These openings have been ignored in this radiation transfer study. As seen in Fig. 5(A), the epidermal cells fit one another like pieces of a jigsaw puzzle.[35] Although one can create different arrangements by varying the way cells are located in space, we tried to define a simple but realistic epidermal layer.[11] Let a_e be the half-axis of the ellipsoid in the plane of the

Table 1. Structural Parameters Defining a Generic Virtual Dicotyledon Leaf[a]

Tissue	Characteristic	Parameter	Value
Epidermis	Cell radius	a_e	12.5*
	Cell oblateness	o_e	0.7
	Cell wall thickness	e_{ce}	1.0*
Palisade parenchyma	Cell radius	a_p	7.5*
	Cell cap oblateness	o_p	1.0
	Cell high	h_p	50*
	Cell wall thickness	e_{cp}	1.0*
	Chloroplast membrane thickness	e_{pp}	1.53
Spongy mesophyll	Basic cell radius	a_s	12
	Fraction of airspaces	ξ_s	0.45*
	Tissue thickness	h_s	50*
	Basic cell wall thickness	e_{cs}	1.0*
	Basic chloroplast membrane thickness	e_{ps}	1.32

[a]Distances are given in micrometers. Values found in the literature are indicated with an asterisk.

leaf (in two directions) and b_e the half-axis of the ellipsoid in the direction perpendicular to the leaf. The roughness of the leaf surface can be easily controlled by the oblateness $o_e = b_e/a_e$ of the ellipsoid. The distance between the centers of two cells along a row is $L_e = \sqrt{3}a_e$, and the distance between two rows of cells is given by $R_e = 3a_e/2$. Each cell is carved out at three symmetric points to leave space for the surrounding cells [Fig. 5(B)]. The volume of one cutout is expressed as follows:

$$2\pi o_e \int_{L_e/2}^{a_e} ({a_e}^2 - x^2)\mathrm{d}x = \frac{16 - 9\sqrt{3}}{12}\,\pi {a_e}^3 o_e, \qquad (1)$$

and the volume V_e of an epidermis cell is given by

$$V_e = \frac{4}{3}\,\pi {a_e}^3 o_e - 3\left(\frac{16 - 9\sqrt{3}}{12}\,\pi {a_e}^3 o_e\right)$$
$$= \frac{27\sqrt{3} - 32}{12}\,\pi {a_e}^3 o_e. \qquad (2)$$

The dashed rectangle in Fig. 5(A) indicates the size of an elementary lattice. Its surface is equal to $S_e = 3\sqrt{3}{a_e}^2$ and contains $N_e = 2$ cells. It is therefore possible to define the volume per unit area $\overline{V_e} = N_e V_e/S_e$ and the fraction of intercellular airspaces in this tissue, i.e., the fraction of space between the epidermis innerside and the palisade parenchyma: $\xi_e = 1 - \overline{V_e}/(2a_e o_e)$. $\xi_e = 25.6\%$ and is independent of the cell size. To define the volume of water V_{we}, we apply the same reasoning. The vacuole membrane has a radius of $a_e - e_{ce}$ and is carved out with ellipsoids of radius $a_e + e_{ce}$, where e_{ce} is the cell wall thickness. The cell wall volume V_{ce} merely equals $V_{ce} = V_e - V_{we}$. It is also easy to express the cell wall volume per unit area ($\overline{V_{ce}}$) and the water volume per unit area ($\overline{V_{we}}$).

2. *Palisade Parenchyma Cells*

As seen before, palisade cells are narrow, cylindrical cells oriented perpendicular to the leaf surface and usually arranged in one or two layers subjacent to the epidermis. Although compactly arranged, they have little mutual contact because of the long, narrow, intercellular voids along their anticlinal walls, as shown in paradermal sections of palisade mesophyll.[11,35,36] The palisade cells have been modeled as cylinders with spherical caps [Fig. 6(A)]. The volume of a single palisade cell V_p is

$$V_p = \pi {a_p}^2\left(h_p + \frac{4a_p o_p}{3}\right), \qquad (3)$$

where a_p is the radius of the palisade cell, o_p is the oblateness of the cylinder cap, and h_p is the height of the cylinder. The oblateness o_p is defined as $o_p =$

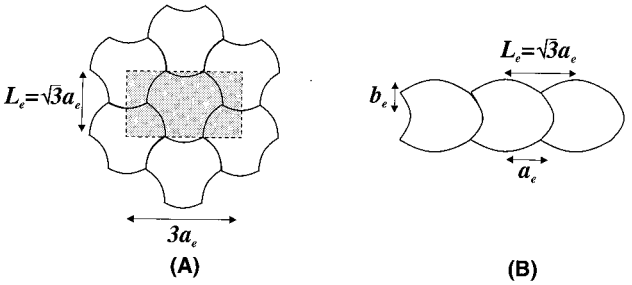

Fig. 5. (A) Top view of the cell arrangement for the epidermis. The shadowed area indicates the elementary lattice. (B) Transverse vertical section of the epidermis.

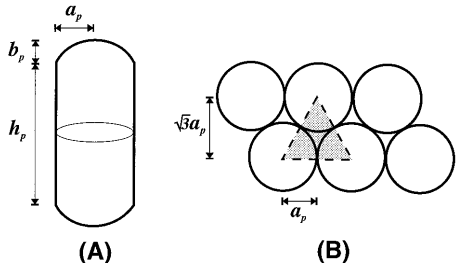

Fig. 6. (A) Palisade cell is made of a cylinder with ellipsoid caps. (B) Paradermal section showing the arrangement in space. The shadowed triangle corresponds to the elementary lattice.

b_p/a_p, where b_p is the half-axis of the cap in the direction perpendicular to the cylinder radius. The triangle in Fig. 6(B) indicates the elementary lattice of area $S_p = \sqrt{3}a_p^2$ that contains $N_p = 1/2$ cell. The volume per unit area $\overline{V_p}$ can be expressed as in the case of the epidermis and the fraction of intercellular airspaces ξ_p as

$$\xi_p = 1 - \frac{\sqrt{3}}{18}\frac{3h_p + 4a_p}{h_p + 2a_p}. \quad (4)$$

One can determine the cell wall volume V_{cp}, as described above, by defining a smaller object whose dimensions are reduced by the cell wall thickness e_{cp}. To evaluate the thickness e_{pp} and volume V_{pp} of the layer containing chlorophyll, we assume that a typical palisade cell contains $n_{pp} = 40$ chloroplasts, each occupying a volume of 85 μm^3.[37,38] One can numerically estimate e_{pp} using the analytical formula of V_{pp}. The remaining volume $V_{wp} = V_p - V_{cp} - V_{pp}$ is filled with water. The volumes per unit area $\overline{V_{cp}}$, $\overline{V_{pp}}$, and $\overline{V_{wp}}$ are easily deduced.

3. Spongy Mesophyll Cells

In contrast to the other two tissues, the shape of spongy mesophyll cells is complex and intercellular airspaces may occupy as much as 50% of the tissue volume. It often appears as a network of cells whose spatial arrangement does not seem to have any regular organization. For that reason, it is almost impossible to describe them by individual volumes. However, the porosity of a typical spongy tissue is isotropic and nondirectional.[14] Consequently, the spongy structure has been modeled by spheres of different sizes, located at random, such that the occupied volume corresponds to observed values. Although this representation is an approximation, it permits a description of the fraction of airspaces such that the isotropy in that tissue is compatible with values found in the literature. Their highly lobed shape mainly enhances gas exchange. Such a statistical approach seems appropriate to describe an irregular tissue that does not appear to obey any simple rule. Furthermore, this approximation is not expected to affect strongly the scattering of light in that layer. We first consider a box of height h_s and base $S_s = 300\ \mu m \times 300\ \mu m$, and assign the volumetric fraction of airspaces ξ_s to 45%. One can generate the spongy mesophyll by filling the box at random with spheres of initial radius a_s without overlapping. When no more space is available, this radius a_s is reduced by 10% and the filling process continues with smaller spheres. This iterative process stops when $1 - \xi_s$ of the space is occupied by cells. A total of 1139 spheres of 11 different sizes allows us to fill the space available at the required density. The thicknesses of all internal membranes of the smaller spheres are similarly decreased. To compute the chloroplast layer thickness of the initial spheres, we assume that the latter contain $n_{ps} = 25$ chloroplasts, each occupying a volume of 85 μm^3, and estimate e_{ps} numerically as for the palisade parenchyma. The remaining volume is then filled with water. This process is repeated for each class of spheres. The spongy cell volume per unit area $\overline{V_s}$ can be expressed as a sum $\Sigma_k\ \overline{V_{s,k}}$ over the 11 different classes of spheres.

4. Generation of the Leaf

The cross section of the leaf appears like a bifacial slab structure, in which the blade is represented as two layers of epidermal cells surrounding a palisade parenchyma and a spongy mesophyll. This organization is of course an idealization of actual leaf structures, which exhibits a rather large natural diversity in the number, shape, and orientation of cells in the various tissues. For example, it has been shown that the palisade cells of *Medicago sativa* leaves do not follow any regular pattern in their arrangement below the epidermal cells[11]: they can be located directly in line with the transverse axis of an epidermal cell, anywhere along the inner periclinal wall, or below a junction of two or more epidermal cells. The boundary between the palisade and spongy mesophyll is also undefined; the small intercellular voids of the palisade mesophyll are continuous with the much larger voids in the subjacent spongy mesophyll, thereby promoting CO_2 diffusion through the whole leaf.

The leaf internal structure is thus fully defined by the 13 parameters summarized in Table 1. The previous formulas allow us to control the fraction of intercellular airspaces, the fractional volume of the different media, as well as the number of cells per square micrometers (N_l), which is given by

$$N_l = \frac{N_e}{S_e} + \frac{N_p}{S_p} + \frac{1}{S_s}\sum N_s + \frac{N_e}{S_e}. \quad (5)$$

Assuming that α_c, α_p, and α_w are the fractional volumes of cell walls, chlorophyllian pigments, and water, respectively, we can also calculate C_c, C_p, C_w, which are the corresponding contents expressed in g cm^{-2} or $\mu g\ cm^{-2}$. The density of water is $v_w = 1.0$ g cm^{-3}, the water content is

$$C_w = v_w(\alpha_{we}\overline{V_e} + \alpha_{wp}\overline{V_p} + \alpha_{ws}\overline{V_s} + \alpha_{we}\overline{V_e}). \quad (6)$$

Table 2 shows that C_w is close to the range of laboratory measurements acquired in the leaf optical properties experiment 93, which yielded a mean value of 0.0115 g cm^{-2} within the 0.0046–0.0405-g cm^{-2} range.[30,39] The case of cell walls is somewhat less straightforward, because of the lack of information about their biophysical properties. Cellulose (including hemicellulose) and lignin are the main constituents of the cell wall, in proportion to 3/4 and 1/4,[30] and they have densities of 1.52 and 1.34.[40] The cell wall density has accordingly been set to $v_c = 1.47$ g cm^{-3}. The biochemical composition of cell walls is almost constant and so is its density. As for cell walls, the water content is expressed as follows:

$$C_c = v_c(\alpha_{ce}\overline{V_e} + \alpha_{cp}\overline{V_p} + \alpha_{cs}\overline{V_s} + \alpha_{ce}\overline{V_e}). \quad (7)$$

As previously, C_c agrees with experimental observations of cellulose plus hemicellulose plus lignin con-

Table 2. Statistics for the Leaf Biophysical Properties

Cell Properties	Parameter	Epidermis	Palisade Parenchyma	Spongy Mesophyll	Whole Leaf
Whole tissue	h (μm)	17.5	65	50	150
	ξ (%)	25.6	16.3	45.0	
	N (cm^{-2})	246,336	513,200	1,265,556	2,271,428
Cell wall	α_c (%)	27.0	26.6	23.0	
	V (μm^3)	1427.51	2815.91	1662.95	
	C_c (g cm^{-2})	0.00052	0.00213	0.00093	0.00410
Pigments	n_p		40	25	
	α_p (%)		32.1	29.4	
	V (μm^3)		3400.00	2125.00	
	C_p (μg cm^{-2})		41.1	19.0	60.1
Water	α_w (%)	73.0	41.4	47.7	
	V (μm^3)	3857.44	4386.96	3450.28	
	C_w (g cm^{-2})	0.00095	0.00225	0.00131	0.00546

tent.[30] Finally, the total leaf chlorophyll content (C_p) is given by

$$C_p = c_p(n_{pp} N_p + \sum n_{ps} N_s), \tag{8}$$

where (n_p) is the average number of chloroplasts in a cell and the chlorophyll content of a chloroplast is $c_p = 2 \times 10^{-6}$ μg. The value of C_p for this modeled leaf is given in Table 2 and appears reasonable.[39] Table 2 also exhibits the other properties of our virtual leaf. For a given set of parameters, one program automatically computes the position of each cell as shown in Fig. 7, and another estimates the statistics developed above. The next step consists in simulating the path of photons through a 300-μm^2 sample of this virtual leaf.

4. Ray-Tracing Principles

One can compute radiation transfer in this virtual three-dimensional leaf with the recently developed Monte Carlo ray-tracing code called RAYTRAN, using the latest computer graphics techniques. This tool was designed to investigate radiation transfer problems in terrestrial environments over a variety of spatial scales.[5,41] Incident rays can be either collimated to simulate direct illumination or distributed angularly to represent diffuse light or both. This permits the representation of natural as well as laboratory lighting conditions. Rays are generated in the forward direction, i.e., from the light source to the scene, and tracked from interaction to interaction throughout the leaf cell structure, until the ray is absorbed or escapes from the leaf. One can calculate the reflectance (R) of a membrane with the Fresnel formulas using the refractive-index differences between two media.[42] The ray is specularly reflected if $u_1 \leq R$, where u_1 is a random number uniformly distributed in [0, 1]; otherwise the ray is refracted in the direction determined by the cosine law of Snell. Given the incident direction Ω_1 and the normal Ω_L to the leaf surface, the direction of reflection $\Omega_2{}^R$ can be expressed as[43]

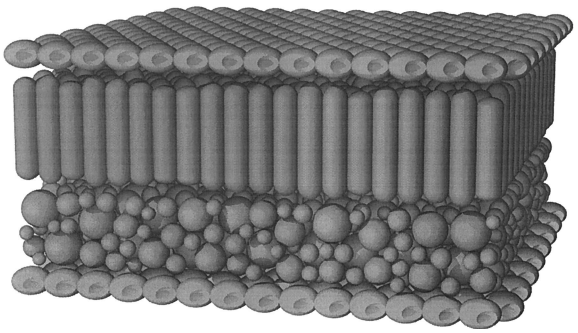

Fig. 7. Perspective view of an artificial dicotyledon leaf. The size of the represented target is 300 μm × 300 μm × 170 μm.

$$\Omega_2{}^R = \Omega_1 - 2(\Omega_L \Omega_1)\Omega_L, \tag{9}$$

and the direction of transmission (refraction) $\Omega_2{}^T$ is given by

$$\Omega_2{}^T = n_{21}\Omega_1 + \Omega_L(n_{21}(-\Omega_L\Omega_1) - \{[1 + n_{21}{}^2(\Omega_L\Omega_1)^2 - 1]\}^{1/2}), \tag{10}$$

where $n_{21} = n_1/n_2$, n_1 is the index of refraction of the medium in which the ray initially propagates, and n_2 is the index of refraction of the intercepted medium. The probability that a ray is absorbed by a medium is defined by Beer's law. The absorption coefficient k of each medium mentioned in Subsection 3.A can be used to estimate the ray free path d_a when it travels in the medium

$$d_a = -\frac{1}{k} \ln u_2, \tag{11}$$

where $u_2 \in [0, 1]$. If d_m is the maximum distance the ray can cover in the medium: it will be absorbed when $d_a < d_m$.

Ray path statistics are accumulated to compute the bidirectional reflectance and transmittance factors, but also the light extinction profile inside the leaf. For the former set of measurements, the hemispheres

above and below the scene are divided into m equal area elementary surfaces S_l. One can use RAYTRAN simply to count how many rays escape through each patch. The bidirectional reflectance factor f_l of the elementary surface S_l is calculated as follows[44]:

$$f_l = \pi \frac{N_l}{N\Delta\Omega_l}, \qquad l = 1, \ldots, m, \tag{12}$$

where N_l represents the number of photons that cross the surface S_l, N is the total number of generated photons, and $\Delta\Omega_l$ is the projected solid angle corresponding to the elementary surface S_l. The bidirectional transmittance factor can be calculated in the same way but one must consider the lower hemisphere. To measure the light fluxes along the normal to the leaf, we regularly positioned 20 virtual detectors along this axis. Each time a ray reaches the upper surface of the sensor, the downward flux counter is incremented by 1; and conversely, the upward flux counter is incremented when a ray reaches its lower surface. Rays collected in this manner are then divided by the total number of emitted rays to provide relative energy fluxes. For each sensor, the relative net flux is calculated as the difference between the downward and upward fluxes. The sampling area is assumed to be surrounded by identical patches in all directions, so that lateral boundary conditions are periodic and the model actually simulates a leaf of infinite extent.

5. Radiative Transfer Simulations

Although the leaf structure described above is greatly simplified compared with that of actual leaves, it nevertheless allows the representation of a fair degree of complexity. The computation of the radiation regime in such a complex medium is not particularly difficult with a ray-tracing model. The number of emitted rays and their initial angular distribution can be set individually for each experiment. The leaf is generated with the parameters shown in Table 1. In addition, to study the effect of the epidermis roughness, we also generated a leaf with an epidermal oblateness $o_e = 0.2$, which represents a smoother surface. In this case, we also increased a_e in order to keep the leaf water content unchanged. We now investigate the spectral behavior and the directional reflectance of this leaf.

A. Spectrum

To evaluate the adequacy of the description of leaf internal structure and optical properties, we calculated the leaf bihemispherical reflectance R_{bh} and transmittance T_{bh} in the 400–2500-nm spectral region at a resolution of 25 nm. The upper (adaxial) face of the leaves is illuminated by an isotropic point light source with a conical angular aperture of 90°. One million rays are generated for each simulated wavelength. The absorptance A_{bh} is derived from the reflectance and the transmittance through the simple relationship $A_{bh} = 1 - (R_{bh} + T_{bh})$. In Fig. 8 one can recognize classic absorption features in the visible (chlorophyll) and the middle infrared (water); the near-IR plateau attributed to leaf internal structure is also well represented. By inversion of the PROSPECT model[30] against these spectra, we estimated the original leaf biophysical parameters. While the retrieved water content (0.00659 g cm^{-2}) is very close to the value of Table 2 (0.00546 g cm^{-2}), the estimated chlorophyll content (18.6 μg cm^{-2}) strongly differs from its actual value (60.1 μg cm^{-2}). This disagreement reveals the limits of a purely refractive scattering approach and the assumption of a homogeneous chlorophyll membrane. The high absorption peak in the red spectral region is not present in the RAYTRAN simulated reflectance spectra. Since increasing the absorption by the chlorophyll pigments does not improve the output of the model, we hypothesized that the discrepancy may be due to an overestimation of the leaf surface reflectance. Consequently, the difference does not necessarily imply a failure of the PROSPECT model. These effects are discussed in more detail in Subsection 5.C. The reflectance and transmittance levels in the near IR are more characteristic of a monocotyledon than a dicotyledon: R_{bh} is underestimated and T_{bh} is overestimated. This bias has been observed before with other models.[12] Decreasing the epidermis roughness to $o_e = 0.2$ mainly affects the transmittance, whereas the reflectance remains almost unchanged. By smoothing out the epidermis, we increased the transmittance of the leaf, except in the spectral region around the peak of water absorption (i.e., ≈1930 nm). In the near-IR spectral region, the slightly higher reflectances associated with the rough epidermis are due to the contribution of multiple scattering. This simulation underscores the role of the epidermis in controlling the internal distribution of light in the leaf structure. These features are investigated further in Subsection 5.B.

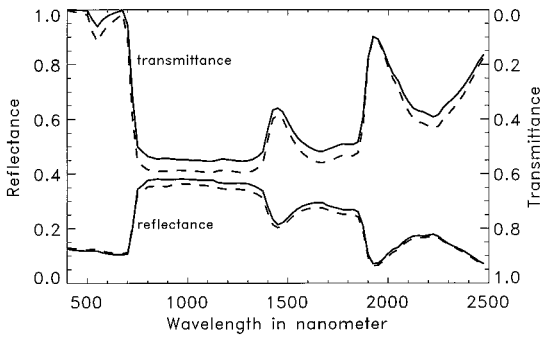

Fig. 8. Leaf bihemispherical reflectance and transmittance. The vertical distance between the two curves represents the absorptance. The solid curve represents the values corresponding to an epidermis with $o_e = 0.7$ and the dashed curve with $o_e = 0.2$.

B. Vertical Light Attenuation

To illustrate the effect of the shape of the epidermis on light scattering, we computed the upward, downward, and net flux with the help of the 20 virtual sensors described at the end of Section 4. Figure 9

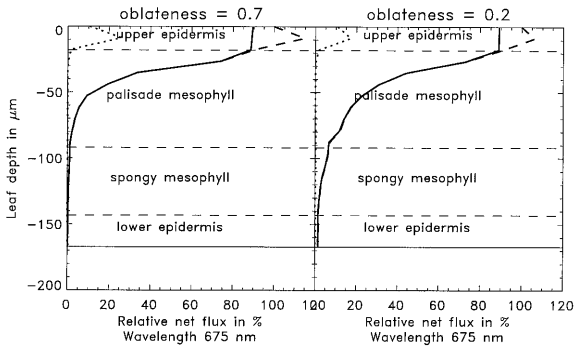

Fig. 9. Relative fluxes perpendicular to the leaf surface: net flux (solid curve), upward flux (dotted curve), downward flux (dashed curve). These fluxes were simulated at a wavelength of 675 nm.

shows the light gradients within the leaf at 675 nm. The simulated attenuation of transmitted light turns out to be close to exponential, indicating significant amounts of absorption. 80% or more of the light is absorbed in the palisade, i.e., within the initial 90 μm or so of the leaf. The extinction of the downward flux is greater in the case of a convex epidermis cell ($o_e = 0.7$). As already observed by many authors,[10,45,46] in an epidermis with convex shape cells, i.e., with a rough surface, each cell acts as a lens that can be used to focus light on the palisade tissue and may affect the absorption. Conversely, when the epidermis is smooth ($o_e = 0.2$), the absorption by the palisade parenchyma tissue appears to be less efficient and the transmittance of the leaf increases. The distribution of light reveals other notable features in accordance with experimental results. For example, small variations in the profiles were observed,[47] when a fiber-optic probe was used, when a transition between two different tissues occurred: these light intensities increase, probably because of optical discontinuities, and can also be seen in Fig. 9. The relative downward flux in the upper epidermis is higher than 100% because the same ray may be scattered several times inside an epidermal cell and hence be counted more than once by a given detector. This concentration of light has already been reported in the literature for various leaves.[6] Figure 9 also shows that the amount of scattered light falls to less than 10% of its initial level within the upper epidermis, as observed experimentally.[47]

C. Hemispherical Reflectance and Transmittance

The relationship between the hemispherical reflectance R_h, or transmittance T_h, and the illumination zenith angle θ_i, assuming collimated radiation, has also been investigated for $\lambda = 675$ and 1000 nm. Results are presented in Fig. 10 for $o_e = 0.7$. In the red spectral region, only R_h varies significantly with θ_i, and then for illumination angles larger than 60°. In the near infrared, R_h and T_h present a similar angular dependency, so that the hemispherical absorptance A_h is essentially constant. The contribution to the reflectance that is due to single scattered rays R_h^s is due entirely to specular reflection and is essentially independent of wavelength, as has been observed before.[48] Calculations of the reflection of light by a dielectric surface in three dimensions using the Fresnel equations and an average refractive index of 1.45 characteristic of leaf material yielded similar results.[49] As the hemispherical single-scattering reflection only results from the surface, it should also be comparable with experimental measurements of the polarized reflectance of plant

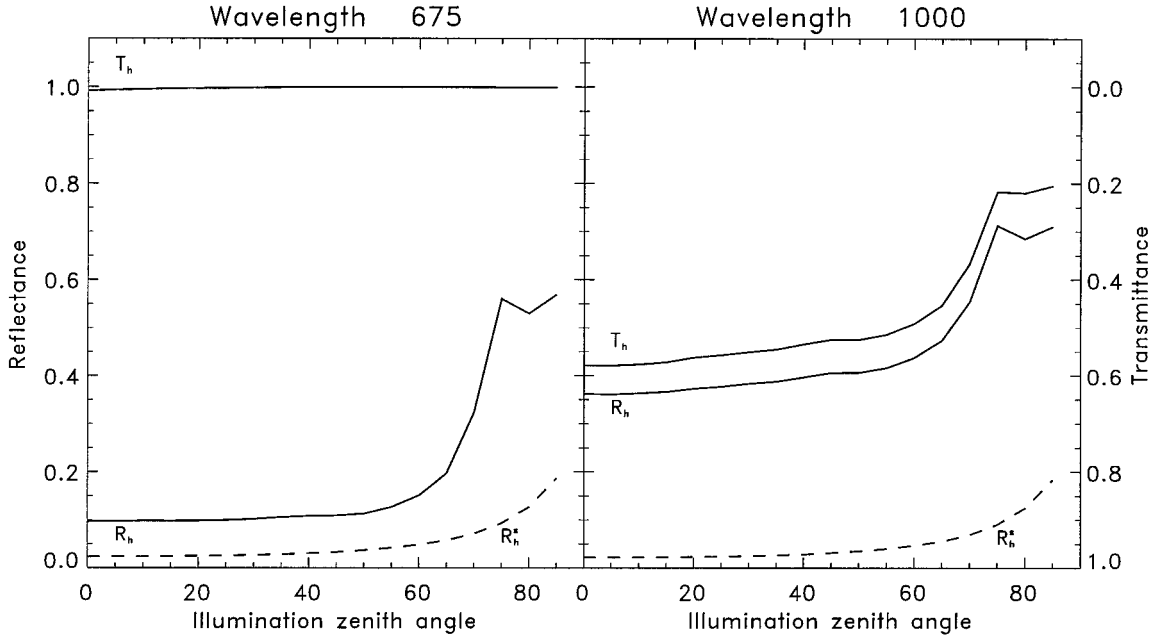

Fig. 10. Hemispherical reflectance R_h, transmittance T_h, and single scattering reflection R_h^s (dashed curve) for various illumination zenith angles ($o_e = 0.7$).

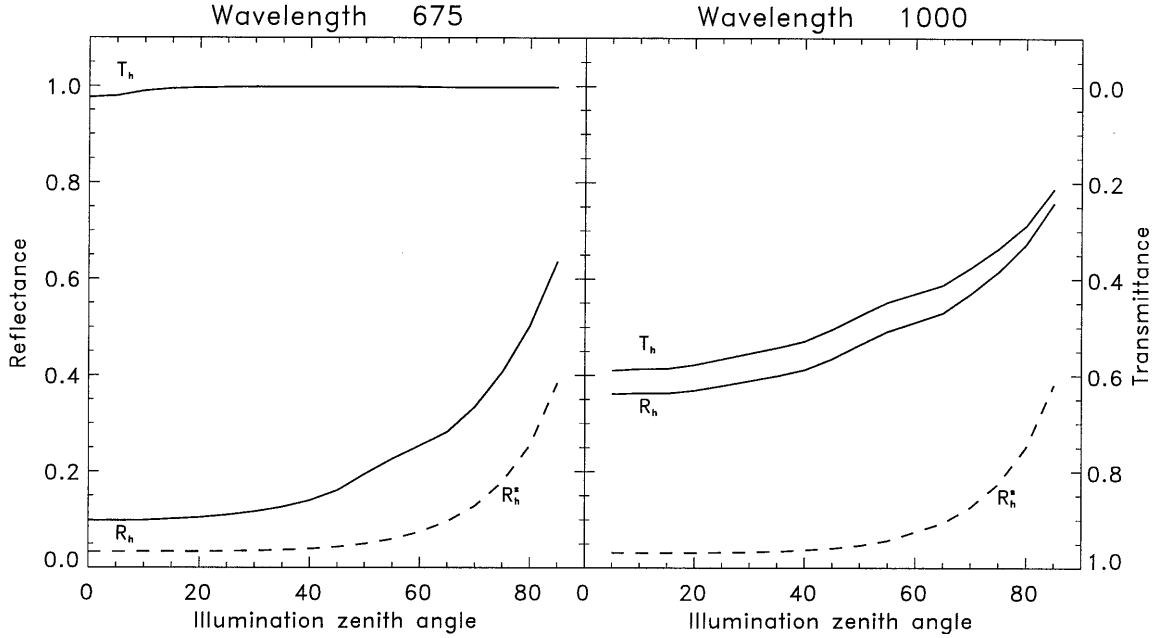

Fig. 11. Hemispherical reflectance R_h, transmittance T_h, and single scattering reflection $R_h{}^s$ (dashed curve) for various illumination zenith angles (o_e = 0.2).

leaves.[29] Because the effects of the cuticular waxes and leaf pubescence (which may produce diffraction and increase $R_h{}^s$) were not explicitly modeled here, our values are relatively low, but still consistent with observations: indeed, the specular reflection rarely exceeds the diffuse reflection in the red spectral region.[50] Typical reflectance values in the red are close to 0.05, with a very weak diffuse component.[48] In our simulation, the diffuse reflection originating from the multiple scattering is somewhat overestimated. Too much of the light transmitted in the epidermis tissue can be scattered back to the upper side. This may be due either to the fact that the actual epidermis absorbs more than what we assumed, or to the neglect of diffraction phenomena. When o_e = 0.2, R_h varies continuously as a function of θ_i, both in the red and near-IR spectral regions (Fig. 11). At high values of θ_i, $R_h{}^s$ becomes large, indicating a strong specular effect.

D. Bidirectional Reflectance and Transmittance

Finally, we simulated the bidirectional reflectance and transmittance for various illumination zenith angles θ_i in the near infrared. The leaves are lighted by a collimated beam generating 10 million rays for each of the three illumination directions (Fig. 12). To avoid any dependence on the azimuth angle of illumination resulting from the regular structure of the epidermis, the reflectances have been averaged for seven illumination azimuth angles, from 0 to 90 deg in steps of 15 deg. Leaves with a rough epidermis have an almost Lambertian reflectance and transmittance. Such Lambertian leaf reflection has already been observed,[51] but most of the leaves exhibit a specular reflection peak.[27,52] To investigate this issue, we experimented with values of o_e varying continuously from 0.7 to 0.2. As the epidermis becomes smoother, the reflectance becomes more specular, especially for high illumination zenith angles. This feature is in accordance with the results of Fig. 11. At large θ_i, the transmittance is also affected by the illumination direction as can be seen in Fig. 12 and reported elsewhere.[48] For oblateness values around 0.3–0.4 and for the particular leaf being modeled here, the specular component exhibits an off-specular peak as predicted by theory.[53] However, more realistic simulations of the leaf bidirectional reflectance will require a careful description of the roughness of the epidermis.

The relation between the reflectance of the leaf and the structure of its epidermis needs to be further investigated. For example, it would be useful to understand why various leaves adopt a particular roughness and how the structure (and hence the radiation transfer characteristics) evolves in space and time. As seen above, convex epidermis cells tend to focus light on the subjacent palisade cells, but also tend to reflect light relatively isotropically. This type of leave is often found in the lower part of the canopy,[10] where direct solar radiation does not easily penetrate. These leaves exhibit a larger absorptance than those with a smoother epidermis and have rather Lambertian bidirectional reflectance. Conversely, leaves with smooth epidermis exhibit a more specular reflectance and absorb less radiation; they are expected to be found in the upper part of the canopy, where direct sunlight is predominant. Through this mechanism, leaves may protect themselves against excessive direct solar radiation and transmit light to the lower layers of the canopy. This mechanism could be ascertained through appropriate field observations.

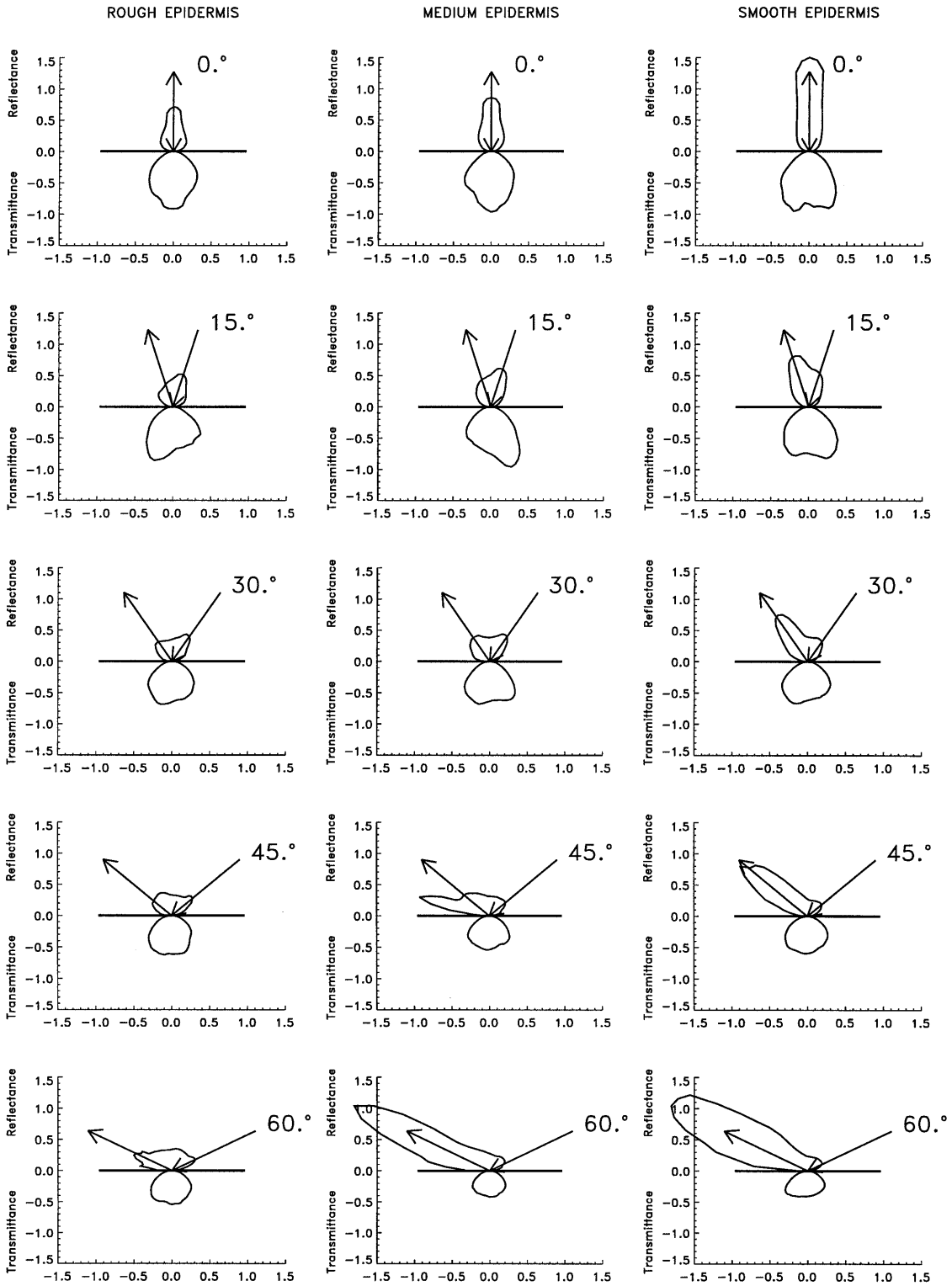

Fig. 12. Bidirectional reflectance and transmittance in the principal plane, in polar coordinates, for illumination angles of 0°, 15°, 30°, 45°, and 60°. The epidermis roughness parameter o_e was set to 0.7, 0.4, and 0.2 for the rough, medium, and smooth cases presented in the left, central, and right columns, respectively.

6. Conclusion

We have reported an innovative attempt to simulate light scattering and absorption in a three-dimensional leaf with a ray-tracing model. The leaf biophysical properties of a typical dicotyledon leaf are reasonably described by its structure, defined as an assemblage of simple geometric volumes filled by three different media: cells wall materials, chlorophyll pigments, and water. The position, size, and shape of each cell in the simulated leaf section are

explicitly defined. These specifications yielded reasonable concentrations of biochemical components. The RAYTRAN model is capable of simulating the spectral and bidirectional properties of such a leaf. Although the model is still in an early stage of development, the results obtained so far agree fairly well with reflectance and transmittance observations. This approach allows us to confirm and improve our understanding of leaf optical properties.

The structure and optical properties of the various leaf tissues have been assigned to conform to the information available in the published literature. The transmittance, reflectance, and absorptance of the leaf were computed with the ray-tracing model, without allowing any further adjustments. In other words, the radiative properties of the simulated dicotyledon leaf described here result exclusively from the geometric description of the leaf tissues, their optical characteristics, and the physical principles of classical optics. Although the general factors controlling absorption and reflection have been understood for a long time, it had never been shown before that a spatially detailed description of leaf structure would yield optical properties as close to the measured ones as those obtained here. Through this rigorous approach, we have succeeded in showing, for the first time to our knowledge, that specific biochemical concentrations in different leaf layers and cell structures could be modeled and to predict actual wavelength-specific light absorption and scattering patterns that closely match observations.

In retrospect, it is interesting to see how important the shape of the epidermis cells is for the transfer of radiation in leaves. The model described above is capable of simulating subtle aspects of this problem, including the focusing of light by these cells on the subjacent tissues. In addition, these initial results suggest new laboratory measurements for which the leaf bidirectional reflectance should be observed simultaneously with the leaf internal structure, in order to investigate the relationships between these two properties. Such an approach would be helpful to improve the representation of leaf directional properties in canopy reflectance models.

The current model excludes a number of leaf tissues and cell types that would make it more physically realistic but would require descriptive information not readily available. For example, conductive tissues are not included, nor are various specialized cells, e.g., schlerids, glands, and trichomes. Additionally, the assumption of a homogeneous chlorophyll membrane may reveal some limitation if finer details of the absorption by chloroplasts are available to investigate the photosynthesis mechanism. Original approaches recently published in the literature[37,33] are worth further investigations. Also of potential interest is the suggestion that the chloroplasts near the upper face of the palisade tissue receive more light than those located near the lower side.[11] Consequently, chloroplasts may develop different strategies to trap light.[46] We also observed that an accurate estimation of the bidirectional reflectance requires accounting for the irregularities in the shape of the epidermis cells. From a physiological point of view, it would also be interesting to examine the light collecting capabilities of various leaf anatomies and chemical compositions. Several authors have already investigated the relationships between leaf spectra and chemical content, but these studies exploit only a limited number of observations.[54,55] Our approach opens the way for new sensitivity studies that may prove useful in the understanding of ecological processes.

The model described here could be improved in various ways to enhance its capability to address those issues. Upgrade priorities should be given to the description of the internal cell structure, to the characterization of the optical properties of the various materials, and to a better representation of ray/object interactions. Each of these classes of ameliorations would improve the accuracy and reliability of the model, at a specific cost. The CSG techniques used to describe the shape of the cells allow us to define much more complex objects for which ray-tracing techniques can always compute the ray/object interception. Since the design of RAYTRAN is independent of the scene, it would be possible to account for more realistic leaf tissues and cell shapes provided the required information is available. However, the more complex the CSG objects, the more computer time is necessary to calculate the ray/object intersections. In addition, the control of artificial leaf construction requires the calculation of volumes of different membranes of the cells. The estimation of the volume of each membrane may no longer be achievable through simple analytical integrals and would require numerical techniques that could make the generation of leaf structure a particularly slow task. Consequently, significant increases in the complexity of the description of the cell structure would require a substantial demand on the computational resources needed to create the leaf and to trace the ray paths. A better characterization of the optical properties of the objects in the modeled scene will require detailed laboratory studies to ascertain the various parameters needed. Finally, improvements in the representation of the physics of radiation transfer could also include an explicit description of scattering processes when the dimension of the scatterers approaches the wavelength of the radiation, the accounting of the phase and polarization of each ray and appropriate parameterizations for those organs not represented explicitly in the virtual leaf (e.g., leaf hair).

Y. M. Govaerts and M. M. Verstraete are grateful for the continuing support of the Space Applications Institute. This research would not have been possible without liberal access to the Centro Svizzero di Calcolo Scientifico in Manno, Switzerland. The contributions of S. Jacquemoud and S. L. Ustin were partly supported by two NASA Earth-Observing System grants NAS5-31359 and NAS5-31714 and by a U.S. Environmental Protection Agency grant

R-821695. They also thank the Digital Equipment Corporation for providing the Alpha computers through the Sequoia 2000 grant number 1243.

References

1. T. C. Vogelmann and L. O. Bjorn, "Plants as light traps," Physiol. Plant. **68,** 704–708 (1986).
2. D. M. Gates, *Biophysical Ecology* (Springer-Verlag, New York, 1980).
3. S. Jacquemoud and F. Baret, "PROSPECT: a model of leaf optical properties spectra," Remote Sensing Environ. **34,** 75–91 (1990).
4. M. M. Verstraete, B. Pinty, and R. Myneni, "Understanding the biosphere from space: strategies to exploit remote sensing data," in *Physical Measurements and Signatures in Remote Sensing* (Val d'Isère, France, 1994), pp. 993–1004.
5. Y. M. Govaerts and M. M. Verstraete, "Evaluation of the capability of BRDF models to retrieve structural information on the observed target as described by a tridimensional ray tracing code," in *Multispectral and Microwave Sensing of Forestry, Hydrology, and Natural Resources*, E. Mougin, K. J. Ranson, and J. A. Smith, eds. Proc. SPIE **2314,** 9–20 (1994).
6. T. C. Vogelmann, "Plant tissue optics," Annu. Rev. Plant Physiol. Plant Mol. Biol. **44,** 231–251 (1993).
7. J. Verdebout, S. Jacquemoud, and G. Schmuck, "Optical properties of leaves: modelling and experimental studies," in *Imaging Spectrometry as a Tool for Environmental Observations*, J. Hill and J. Mégier, eds. (Kluwer Academic, Dordrecht, The Netherlands, 1994), pp. 169–191.
8. G. Haberlandt, "Optical sense-organs," in *Physiological Plant Anatomy*, G. Haberlandt, ed. (Macmillan, London, 1914), pp. 613–631.
9. H. Gabrys-Mizera, "Model considerations of the light conditions in noncylindrical plant cells," Photochem. Photobiol. **24,** 453–461 (1976).
10. R. A. Bone, D. W. Lee, and J. M. Norman, "Epidermal cells functioning as lenses in leaves of tropical rain-forest shade plants," Appl. Opt. **24,** 1408–1412 (1985).
11. G. Martin, S. A. Josserand, J. F. Bornman, and T. C. Volgemann, "Epidermal focussing and the light microenvironment within leaves of Medicago sativa," Physiol. Plant. **76,** 485–492 (1989).
12. W. A. Allen, H. W. Gausman, and A. J. Richardson, "Willstatter-Stoll theory of leaf reflectance evaluated by ray tracing," Appl. Opt. **12,** 2448–2452 (1973).
13. R. Kumar and L. Silva, "Light ray tracing through a leaf cross section," Appl. Opt. **12,** 2950–2954 (1973).
14. D. F. Parkhurst, "Internal leaf structure: a three-dimensional perspective," in *On the Economy of Plant Form and Function*, T. J. Givnish, ed. (Cambridge U. Press, Cambridge, U.K., 1986), pp. 215–249.
15. T. C. Vogelmann and G. Martin, "The functional significance of palisade tissue penetration of directional versus diffuse light," Plant Cell Environ. **16,** 65–72 (1993).
16. D. F. Parkhurst, "Stereological methods for measuring internal leaf structure variables," Am. J. Bot. **69,** 31–39 (1982).
17. L. J. Gibson and M. F. Ashby, *Cellular Solids, Structure and Properties* (Pergamon, Oxford, 1988).
18. H. Mohr and P. Schopfer, *Plant Physiology* (Springer-Verlag, Berlin, 1995).
19. D. M. Gates, H. J. Keegan, J. C. Schleter, and V. R. Weiner, "Spectral properties of plants," Appl. Opt. **4,** 11–20 (1965).
20. T. R. Sinclair, M. M. Schreiber, and R. M. Hoffer, "Diffuse reflectance hypothesis for the pathway of solar radiation through leaves," Agron. J. **65,** 276–283 (1973).
21. H. K. Lichtenthaler, "Chlorophylls and carotenoids: pigments of photosynthetic biomembranes," Methods Enzymol. **148,** 350–382 (1987).
22. R. L. Hulbary, "The influence of air spaces on the three-dimensional shapes of cells in Elodea stems, and a comparison with pith cells of Ailanthus," Am. J. Bot. **31,** 561–580 (1944).
23. D. W. Thompson, *On Growth and Form* (Cambridge U. Press, Cambridge, U.K., 1961).
24. J. A. Romberger, Z. Hejnowicz, and J. F. Hill, *Plant Structure: Function and Development* (Springer-Verlag, Berlin, 1993).
25. M. E. Mortenson, *Geometric Modeling* (Wiley, New York, 1985).
26. H. T. Breece and R. A. Holmes, "Bidirectional scattering characteristics of healthy green soybeans and corn leaves *in vivo*," Appl. Opt. **10,** 119–127 (1971).
27. T. W. Brakke, J. A. Smith, and J. M. Harnden, "Bidirectional scattering of light from tree leaves," Remote Sensing Environ. **29,** 175–183 (1989).
28. E. A. Walter-Shea, J. M. Norman, and B. L. Blad, "Leaf bidirectional reflectance and transmittance in corn and soybean," Remote Sensing Environ. **29,** 161–174 (1989).
29. L. Grant, C. S. T. Daughtry, and V. C. Vanderbilt, "Polarized and specular reflectance variation with leaf surface features," Physiol. Plant. **88,** 1–9 (1993).
30. S. Jacquemoud, S. L. Ustin, J. Verdebout, G. Schmuck, G. Andreoli, and B. Hosgood, "Estimating leaf biochemistry using the PROSPECT leaf optical properties model," Remote Sensing Environ. **56,** 194–202 (1996).
31. J. A. Curcio and C. C. Petty, "The near infrared absorption spectrum of liquid water," J. Opt. Soc. Am. **41,** 302–304 (1951).
32. K. F. Palmer and D. Williams, "Optical properties of water in the near infrared," J. Opt. Soc. Am. **64,** 1107–1110 (1974).
33. T. Richter and L. Fukshansky, "Authentic *in vivo* absorption spectra for chlorophyll in leaves as derived from *in situ* and *in vitro* measurements," Photochem. Photobiol. **59,** 237–247 (1994).
34. Q. Ma, A. Ishimaru, P. Phu, and Y. Kuga, "Transmission, reflection and depolarization of an optical wave for a single leaf," IEEE Trans. Geosci. Remote Sensing **28,** 865–872 (1990).
35. K. J. Niklas, *Plant Biomechanics: an Engineering Approach to Plant Form and Function* (University of Chicago Press, Chicago, Ill., 1992).
36. K. Esau, *Plant Anatomy* (Wiley, New York, 1965).
37. L. Fukshansky, V. Martinez, A. Remisowsky, J. McClendon, A. Ritterbush, T. Richter, and H. Mohr, "Absorption spectra of leaves corrected for scattering and distributional error: a radiative transfer and absorption statistics treatment," Photochem. Photobiol. **57,** 538–555 (1993).
38. P. N. Schurhoff, "Die Plastiden," in *Handbuch der Pflanzenanatomie* (Gebrüder Borntraeger, Berlin, 1924).
39. B. Hosgood, S. Jacquemoud, G. Andreoli, J. Verdebout, G. Pedrini, and G. Schmuck, "Leaf optical properties experiment 93 (LOPEX93)," Technical Report EUR 16095 EN (European Commission, Joint Research Centre, Institute for Remote Sensing Applications, Ispra, Italy, 1995).
40. A. J. Stamm and H. T. Sanders, "Specific gravity of the wood substance of loblolly pine as affected by chemical composition," Tappi **49,** 397–400 (1966).
41. Y. M. Govaerts and M. M. Verstraete, "Applications of the L-systems to canopy reflectance modeling in a Monte Carlo ray tracing technique," in *Fractals in Geoscience and Remote Sensing*, G. G. Wilkinson, L. Kanellopoulos, and J. Mégier, eds. (Joint Research Centre of the European Commission, Ispra, Italy, 1994), pp. 211–236.
42. M. Born and E. Wolf, *Principles of Optics*, 2nd ed. (Pergamon, Oxford, 1964).
43. A. S. Glassner, "Surface physics for ray tracing," in *Introduc-*

tion to Ray Tracing, A. S. Glassner, ed. (Academic, London, 1989), pp. 121–160.
44. J. K. Ross and A. L. Marshak, "The influence of leaf orientation and the specular component of leaf reflectance on the canopy bidirectional reflectance," Remote Sensing Environ. **27,** 251–260 (1989).
45. D. W. Lee, "Unusual strategies of light absorption in rainforest herbs," in *On the Economy of Plant Form and Function*, T. J. Givnish, ed. (Cambridge U. Press, Cambridge, U.K., 1986), pp. 105–131.
46. M. E. Poulson and T. C. Vogelmann, "Epidermal focussing and effects upon photosynthetic light-harvesting in leaves of oxalis," Plant Cell Environ. **13,** 803–811 (1990).
47. T. C. Vogelmann, J. F. Bornman, and S. Josserand, "Photosynthetic light gradients and spectral régime within leaves of *Medicago sativa*," Philos. Trans. R. Soc. London Ser. B **323,** 411–421 (1989).
48. T. W. Brakke, "Specular and diffuse components of radiation scattered by leaves," Agri. Forest Meteorol. **71,** 283–295 (1994).
49. W. A. Allen, "Transmission of isotropic light across a dielectric surface in two and three dimensions," J. Opt. Soc. Am. **63,** 664–666 (1973).
50. J. H. McClendon, "The micro-optics of leaves. I. Patterns of reflection from the epidermis," Am. J. Bot. **71,** 1391–1397 (1984).
51. T. W. Brakke, "Goniometric measurements of light scattered in the principal plane from leaves," in *International Geoscience and Remote Sensing Symposium* (IEEE, New York, 1992), pp. 508–510.
52. T. W. Brakke, W. P. Wergin, E. F. Erbe, and J. M. Harnden, "Seasonal variation in the structure and red reflectance of leaves from yellow poplar, red oak, and red maple," Remote Sensing Environ. **43,** 115–130 (1993).
53. K. E. Torrance and E. M. Sparrow, "Theory for off-specular reflection from roughened surfaces," J. Opt. Soc. Am. **57,** 1105–1114 (1967).
54. F. Baret, S. Jacquemoud, G. Guyot, and C. Leprieur, "Modeled analysis of the biophysical nature of spectral shifts and comparison with information content of broad bands," Remote Sensing Environ. **41,** 133–142 (1992).
55. F. M. Danson, M. D. Steven, T. J. Malthus, and J. A. Clark, "High-spectral resolution data for determining leaf water content," Int. J. Remote Sensing **13,** 461–470 (1992).